ISME

Analysis of Multiple Yoffe-Type Moving Cracks in an Orthotropic Half-Plane under Mixed Mode Loading Condition

R. Sourki[*]
PhD Student

M. M. Monfared[†]
Assistant Professor

R. Yaghoubi[‡]
M.Sc. Student

The present paper deals with the mixed mode fracture analysis of a weakened orthotropic half-plane with multiple cracks propagation. The orthotropic half-plane contains Volterra type glide and climb edge dislocations. It is assumed that the medium is under in-plane loading conditions. The distributed dislocation technique is used to obtain integral equations for the dynamic problem of multiple smooth cracks which are located in an orthotropic half-plane. At first, with the help of Fourier transform the dislocation problem is solved and the stress fields are obtained. The integral equations are of Cauchy type singularity and are solved numerically to obtain the dislocation densities on the surface of several cracks to determine the dynamic stress intensity factors on the crack tips. Several numerical examples are solved to evaluate mode I and mode II dynamic stress intensity factors to show the effects of the orthotropy parameters, crack lengths, and crack speed on the dynamic stress intensity factors.

Keywords: Mixed mode, Dynamic stress intensity factors, Multiple cracks, Distributed dislocation technique

1 Introduction

In manufacturing processes a large number of materials in the form of composites, orthotropic and isotropic materials are utilized. Orthotropic materials, due to their wide usage in industries and their wide accessibilities in nature, for instance woods, rolled metals, and diverse crystals, are used in structures and have drawn a great deal of attention in the last several decades. These materials, however, are not produced perfectly and contain a good deal of imperfections such as dislocations, pores as well as vacancies making them vulnerable to cracking.
Unfortunately, cracks, as one of the most important kind of imperfections, cause materials to fail catastrophically. Cracks, also, have a devastating effect on structures which restricts their lives and might cause safety issues. As a result, the study of fracture mechanics in orthotropic

[*] PhD Student, 1) Faculty of Engineering, University of Zanjan, Zanjan, Iran; 2) Faculty of Applied Science, School of Engineering, The University of British Columbia, Canada, rsourki@gmail.com
[†] Corresponding Author, Assistant Professor, Department of Mechanical Engineering, Hashtgerd Branch, Islamic Azad University, P.O. Box 33615-178, Alborz, Iran, mo_m_monfared@yahoo.com
[‡] M.Sc. Student, Department of Mechanical Engineering, University of Tarbiat Modares, Tehran, Iran, goler_1993@yahoo.com

materials is very significant which boils down to the investigation of the crack propagation, including the dynamic problems.

The study of the dynamic problem has drawn a great attention which has been tackled by many researchers in the last decades. For instance, Rubio-Gonzalez and Mason [1] studied the stress intensity factors for a semi-infinite crack in an infinite orthotropic material under impact loads. As expected, they have found that the stress intensnity factors are proportional to the square root of time. Wang et al. [2] have studied the transient elastodynamic response of an orthotropic material under concentrated shear impact loads and have found the DSIFs for the orthotropic materials as well as for an isotropic material. Li and Guo [3] investigated the effects of nonhomogeneity parameter on the DSIFs under anti-plane shear impact loads. It is indicated that the SIFs are highly dependent on the nonhomogeneity parameter. Itou [4, 5] has investigated the transient stresses around a cylindrical crack in an infinite elastic medium subject to impact loads and a crack at interface between half-planes and layers with continuous material properties. Xu et al. [6] studied the plane strain problem of semi-infinite cracks in an infinite functionally graded orthotropic material under uniform impact loading. Dynamically analysis of a crack in an infinite functionally graded strip for anti-plane crack problem under impact loading was investigated by Zhao et al. [7].

In this investigation, they have found that by decreasing inhomogeneous coefficients and increasing the gradient parameter, the DSIFs goes down dramatically. Transient problem of weakened mediums were also of great interests among researchers. As an example, Rubio-Gonzalez and Mason [8, 9] have investigated the elastodynamic response of an infinite orthotropic material with finite crack under normal and tangent concentrated loads and also investigated the crack propagation at constant speed. Ma and Chen [10] studied the transient problem of a half-space weakened by a inclined semi-infinite crack under dynamic anti-plane loading. The DISFs were obtained numerically. The transient stress intensity factors for mode I of a penny-shaped crack in an infinite poroelastic solid has been investigated by Jin and Zhong [11] in which it is found that the dynamic stress intensity factor of poroelastic medium is smaller than that of elastic medium. Zhang et al. [12] studied a transient dynamic crack analysis for functionally graded material. In this work, they have analyzed the effects of the material gradients on the transient DSIFs. Itou [13] studied the transient dynamic stresses around three stacked parallel crack in an infinite elastic plate for an incident impact stress wave impinging normal to the cracks. Antipov and Smirnov [14] studied the two dimensional transient problem of a semi-infinite crack which is propagating at constant speed under time independent loading in the interface of an isotropic infinite strip and an isotropic half-plane. The effects of boundary conditions and weight functions on stress intensity factors were discussed. Ma et al. [15] investigated a Yoffe type finite crack with constant length propagating in the FG strip under the plane loading. In this paper, the effects of material properties, the thickness of the FG strip, and speed of the crack propagating on the dynamic fracture behavior are investigated. In another work, Ma et al. [16, 17] have studied a Yoffe type finite crack propagating in the FG orthotropic medium as well as a strip under plane and anti-plane loading conditions respectively. They have shown that the effects of material properties and the speed of the crack propagating upon the dynamic fracture behavior are significant. Song and Paulino [18] investigated the DSIFs for both homogeneous and nonhomogeneous mediums under dynamic loadings. Ashbaugh [19] determined the stress intensity factors for a finite crack, with an arbitrary orientation and distance from the boundary, under uniform pressure and uniform shear stress. Aijun [20] studied a dynamic stress intensity factors of circular disk with a radial edge crack under impulsive pressure. It is found that the stress intensity factors vary periodically with time under sudden step external pressure.

Malekzadeh Fard et al. [21] investigated the DSIFs for a half-plane which is weakened by multiple finite moving cracks. In this investigation, the influence of crack length and crack running velocity on the stress intensity factors found to be significant.
Wang et al. [22] have investigated the DSIFs for homogenous and nonhomogeneous materials under dynamic loadings which is shown that these parameters have important effects on the DSIFs. Ma et al. [23] analyzed the DSIFs for a Griffith crack in functionally graded orthotropic materials under time harmonic loading. In this study, material properties and the crack configuration on the DSIFs are shown to be highly effective. Monfared and Ayatollahi [24, 25] have investigated the DSIFs of multiple cracks in the functionally graded orthotropic half-plane and strip with FGM coating under time-harmonic loadings. In these studies they have found that the material properties and crack configurations play a momentous role on the DSIFs. Itou [26, 27] investigated the dynamic stresses around two equal collinear cracks in an infinite elastic medium and found stresses around a crack in an infinite elastic strip based on linearized couple-stress theory under time-harmonic stress waves and uniform tension loadings. In another study, Itou [28] investigated the DSIFs around three collinear cracks in an infinite orthotropic plate under time harmonic elastic waves impinging perpendicularly to the cracks.
The aim of this paper is to study the mixed mode dynamic stress intensity factors for cracks propagation in an orthotropic half-plane under in-plane loadings analytically. The Fourier transform is employed to obtain integral forms for the displacements and stress fields. The distributed dislocation technique is utilized to analyze multiple cracks propagation with various speeds and lengths. Then, singular integral equations for multiple cracks propagation are obtained. Several numerical examples are solved to study the effects of material properties, crack length and the velocity of crack on the DSIFs

2 Stress analysis under edge dislocations

A half-plane made of orthotropic materials weakened by Volterra types climb and glide edge dislocations is shown in Figure (1) under the in-plane deformation, the constitutive equations of the orthotropic materials in a fixed Cartesian coordinate system (X, Y) may be expressed as

$$\begin{aligned}
\sigma_{XX}(X,Y) &= C_{11}\frac{\partial u}{\partial X} + C_{12}\frac{\partial v}{\partial Y},\\
\sigma_{YY}(X,Y) &= C_{12}\frac{\partial u}{\partial X} + C_{22}\frac{\partial v}{\partial Y},\\
\sigma_{XY}(X,Y) &= C_{66}\left(\frac{\partial u}{\partial Y} + \frac{\partial v}{\partial X}\right).
\end{aligned} \tag{1}$$

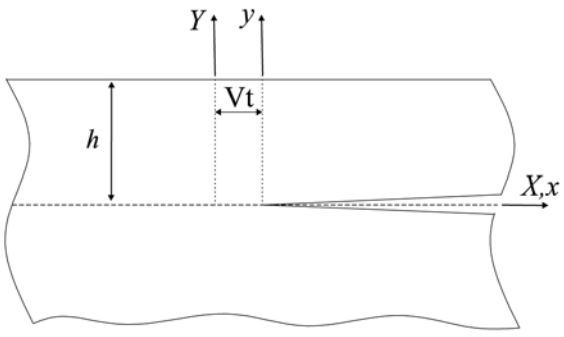

Figure 1 Geometry of an orthotropic half plane with glide and climb dislocations

In the above equalities, C_{11}, C_{22}, C_{12} and C_{66} stand for the elastic stiffness constants. By virtue of Eq. (1) and the equations of motion, $\sigma_{ij,j} = \rho \ddot{u}_i$, we have

$$\begin{aligned} C_{11}\frac{\partial^2 u}{\partial X^2} + C_{66}\frac{\partial^2 u}{\partial Y^2} + (C_{66}+C_{12})\frac{\partial^2 v}{\partial X \partial Y} &= \rho \frac{\partial^2 u}{\partial t^2}, \\ C_{66}\frac{\partial^2 v}{\partial X^2} + C_{22}\frac{\partial^2 v}{\partial Y^2} + (C_{66}+C_{12})\frac{\partial^2 u}{\partial X \partial Y} &= \rho \frac{\partial^2 v}{\partial t^2}. \end{aligned} \tag{2}$$

Where ρ is the elastic material density. For a propagating dislocation depicted in Figure (1), the transformed coordinates can be written as follows.

$$X = x + Vt, \quad y = Y, \quad \frac{\partial^2 .}{\partial t^2} = V^2 \frac{\partial^2 .}{\partial x^2}. \tag{3}$$

In the above mentioned equation (x, y) is the translating coordinate system, which is connected to the crack surface, and *V* is the crack speed along the *X*-axis. By view of Eq. (3), Eq. (2) can be written in terms of the moving coordinate system (x, y) as

$$\begin{aligned} \alpha_1 \frac{\partial^2 u}{\partial x^2} + \frac{\partial^2 u}{\partial y^2} + \alpha_2 \frac{\partial^2 v}{\partial x \partial y} &= 0, \\ \alpha_4 \frac{\partial^2 v}{\partial x^2} + \alpha_3 \frac{\partial^2 v}{\partial y^2} + \alpha_2 \frac{\partial^2 u}{\partial x \partial y} &= 0. \end{aligned} \tag{4}$$

in which

$$\alpha_1 = \frac{C_{11}}{C_{66}} - c^2, \ \alpha_2 = \frac{C_{12}}{C_{66}} + 1, \ \alpha_3 = \frac{C_{22}}{C_{66}}, \ \alpha_4 = 1 - c^2.$$

Where $c = V/C_{sh}$ and C_{sh} is the shear wave speed of the orthotropic half-plane which is given by

$$C_{sh} = \sqrt{C_{66}/\rho} \tag{5}$$

The dislocation cut created along the positive direction of the x-axis. Also, climb and glide edge dislocations are shown with Burger vectors b_y and b_x respectively, which have been located at the origin of the coordinate system. Therefore, the conditions representing the dislocation may be written as

$$\begin{aligned} v(x,0^+) - v(x,0^-) &= b_y H(x), \\ u(x,0^+) - u(x,0^-) &= b_x H(x). \end{aligned} \tag{6}$$

Where $H(.)$ is the Heaviside step function. The stress components must be continuous along the dislocation cut, consequently, we have

$$\begin{aligned}\sigma_{yy}(x,0^+) &= \sigma_{yy}(x,0^-),\\ \sigma_{xy}(x,0^+) &= \sigma_{xy}(x,0^-), \qquad |x| < \infty.\end{aligned} \tag{7}$$

The traction-free conditions on the boundary of half-plane yields

$$\begin{aligned}\sigma_{yy}(x,h) &= 0,\\ \sigma_{xy}(x,h) &= 0.\end{aligned} \tag{8}$$

By applying complex Fourier transform to the system of Eq. (4) we have

$$\begin{aligned}&\frac{d^2U^*}{dy^2} - is\alpha_2\frac{dV^*}{dy} - s^2\alpha_1U^* = 0,\\ &\alpha_3\frac{d^2V^*}{dy^2} - is\alpha_2\frac{dU^*}{dy} - s^2\alpha_4V^* = 0.\end{aligned} \tag{9}$$

Where s is the transform variable and

$$U^*(s,y) = \int_{-\infty}^{\infty} u(x,y)e^{isx}dx,$$

$$V^*(s,y) = \int_{-\infty}^{\infty} v(x,y)e^{isx}dx. \tag{10}$$

Since the displacement components must vanish for $y \to -\infty$, the solution of Eq. (9) may be expressed as follow

$$\begin{cases} U_1^*(s,y) = \sum_{j=1}^{4} m_j(s)B_j(s)e^{\lambda_j y}, \\ V_1^*(s,y) = \sum_{j=1}^{4} B_j(s)e^{\lambda_j y}, 0 \le y \le h \end{cases}, \quad \begin{cases} U_2^*(s,y) = \sum_{j=3}^{4} m_j(s)B_{j+2}(s)e^{\lambda_j y}, \\ V_2^*(s,y) = \sum_{j=3}^{4} B_{j+2}(s)e^{\lambda_j y}, y \le 0. \end{cases} \tag{11}$$

in which $A_j(s), j = 1,2,3,4$ and $\lambda_j(s), j = 1,2,3,4$ are unknown functions and the roots of the following characteristic equation derived from Eq. (9), respectively

$$\lambda^4 + \frac{s^2}{\alpha_3}[\alpha_2^2 - \alpha_1\alpha_3 - \alpha_4]\lambda^2 + \frac{\alpha_1\alpha_4}{\alpha_3}s^4 = 0 \tag{12}$$

The roots of the characteristic equation are given by

$$\lambda_3(s) = -\lambda_1(s) = |s|\lambda_{11},\ \lambda_4(s) = -\lambda_2(s) = |s|\lambda_{22}. \tag{13}$$

where

$$\begin{aligned}\lambda_{11} &= \frac{1}{\sqrt{2\alpha_3}}[\alpha_1\alpha_3 + \alpha_4 - \alpha_2^{\,2} - \sqrt{(\alpha_1\alpha_3 + \alpha_4 - \alpha_2^{\,2})^2 - 4\alpha_1\alpha_3\alpha_4}]^{\frac{1}{2}},\\ \lambda_{22} &= \frac{1}{\sqrt{2\alpha_3}}[\alpha_1\alpha_3 + \alpha_4 - \alpha_2^{\,2} + \sqrt{(\alpha_1\alpha_3 + \alpha_4 - \alpha_2^{\,2})^2 - 4\alpha_1\alpha_3\alpha_4}]^{\frac{1}{2}}.\end{aligned} \tag{14}$$

The coefficients $m_j(s), j=1,2,3,4$ for roots $\lambda_j(s)$ can be expressed as

$$m_j(s)=\frac{is\alpha_2\lambda_j(s)}{\lambda_j^2(s)-s^2\alpha_1} \tag{15}$$

By applying the Fourier transform to the aforementioned conditions, Eqs. (6) to (8), we have

$$\begin{aligned}
&m_{11}B_1(s)+m_{22}-m_{11}B_3(s)-m_{22}B_4(s)+m_{11}B_5(s)+m_{22}B_6(s)=i\,\mathrm{sgn}(s)b_x(\pi\delta(s)+i/s),\\
&B_1(s)+B_2(s)+B_3(s)+B_4(s)-B_5(s)-B_6(s)=b_y(\pi\delta(s)+i/s),\\
&-d_1B_1(s)-d_2B_2(s)+d_1B_3(s)+d_2B_4(s)-d_1B_5(s)-d_2B_6(s)=0,\\
&d_3B_1(s)+d_4B_2(s)+d_3B_3(s)+d_4B_4(s)-d_3B_5(s)-d_4B_6(s)=0,\\
&-d_1e^{-|s|\lambda_{11}h}B_1(s)-d_2e^{-|s|\lambda_{22}h}B_2(s)+d_1e^{|s|\lambda_{11}h}B_3(s)+d_2e^{|s|\lambda_{22}h}B_4(s)=0,\\
&d_3e^{-|s|\lambda_{11}h}B_1(s)+d_4e^{-|s|\lambda_{22}h}B_2(s)+d_3e^{|s|\lambda_{11}h}B_3(s)+d_4e^{|s|\lambda_{22}h}B_4(s)=0.
\end{aligned} \tag{16}$$

Where $\mathrm{sgn}(.)$ is the sign function, $\delta(.)$ is the Dirac delta function and

$$\begin{aligned}
&m_{11}=\frac{\alpha_2\lambda_{11}}{\lambda_{11}^2-\alpha_1}, m_{22}=\frac{\alpha_2\lambda_{22}}{\lambda_{22}^2-\alpha_1}, d_1=(\alpha_2-1)m_{11}+\alpha_3\lambda_{11},\\
&d_2=(\alpha_2-1)m_{22}+\alpha_3\lambda_{22}, d_3=m_{11}\lambda_{11}-1,
\end{aligned}$$

and $d_4=m_{22}\lambda_{22}-1$. By solving Eqs. (16), six unknown functions $B_i(s), i=1,2,...,6$ will be determined which are given in **Appendix A**.

Substituting the determined functions into Eqs. (11) and applying Fourier inverse transform the displacement fields are obtained as the follow

$$u(x,y)=\frac{1}{\pi}\int_0^\infty\{T_u^{11}[T_u^{12}+T_u^{13}+T_u^{14}+T_u^{15}]b_x\sin(sx)+T_u^{21}[T_u^{22}+T_u^{23}+T_u^{24}+T_u^{25})]b_y\cos(sx)\}ds$$

$$v(x,y)=\frac{1}{\pi}\int_0^\infty\{T_v^{11}[T_v^{12}+T_v^{13}+T_v^{14}+T_v^{15}]b_x\cos(sx)+T_v^{21}[T_v^{22}+T_v^{23}+T_v^{24}+T_v^{25}]b_y\sin(sx)\}ds \tag{17}$$

in which T_u^{ij} and T_v^{ij} are given in **Appendix B.**

By using Eqs. (18) and Eq. (1) the stress components may be stated as

$$\begin{aligned}
\sigma_{xx}(x,y)&=S_{xx}^{11}\{S_{xx}^{12}-S_{xx}^{13}-S_{xx}^{14}+S_{xx}^{15}+S_{xx}^{16}-S_{xx}^{17}\}b_x+S_{xx}^{21}\{S_{xx}^{22}+S_{xx}^{23}-S_{xx}^{24}+S_{xx}^{25}-S_{xx}^{26}+S_{xx}^{27}\}b_y\\
\sigma_{yy}(x,y)&=S_{yy}^{11}\{S_{yy}^{12}-S_{yy}^{13}-S_{yy}^{14}+S_{yy}^{15}+S_{yy}^{16}-S_{yy}^{17}\}b_x+S_{yy}^{21}\{S_{yy}^{22}+S_{yy}^{23}-S_{yy}^{24}+S_{yy}^{25}-S_{yy}^{26}+S_{yy}^{27}\}b_y\\
\sigma_{xy}(x,y)&=S_{xy}^{11}\{S_{xy}^{12}+S_{xy}^{13}-S_{xy}^{14}+S_{xy}^{15}+S_{xy}^{16}-S_{xy}^{17}\}b_x+S_{xy}^{21}\{S_{xy}^{22}+S_{xy}^{23}+S_{xy}^{24}+S_{xy}^{25}+S_{xy}^{26}+S_{xy}^{27}\}b_y
\end{aligned} \tag{18}$$

where functions $S_{ij}^{kl};i,j=x,y;\ k,l=1,2$ are given in **Appendix C.**

From Eq. (18), we may observe that stress components exhibit the familiar Cauchy-type singularity at dislocation location.

3 Half-plane under point load

In this section, the orthotropic half plane is subjected to in plane point load with magnitude σ_0 and τ_0 applied on the boundary. As a consequence, the boundary conditions may be written as

$$\sigma_{yy}(x,h) = \sigma_0 \delta(x), \qquad \sigma_{xy}(x,h) = \tau_0 \delta(x). \tag{19}$$

where $\delta(.)$ is the Dirac delta function. By applying the Fourier transform to the above mentioned conditions, and solving Eq. (9) by virtue of Eq. (11), performing a procedure similar to the dislocation solution will result in the following displacements

$$v(x,y) = \frac{1}{\pi}\int_0^\infty \frac{1}{sC_{66}}\{\tau_0[\frac{d_1 e^{s\lambda_{22}(y-h)} - d_2 e^{s\lambda_{11}(y-h)}}{d_2 d_3 - d_1 d_4}]\sin(sx) + \sigma_0[\frac{d_3 e^{s\lambda_{22}(y-h)} - d_4 e^{s\lambda_{11}(y-h)}}{d_2 d_3 - d_1 d_4}]\cos(sx)\}ds$$

$$u(x,y) = \frac{1}{\pi}\int_0^\infty \frac{1}{sC_{66}}\{\sigma_0[\frac{d_3 m_{22} e^{s\lambda_{22}(y-h)} - d_4 m_{11} e^{s\lambda_{11}(y-h)}}{d_2 d_3 - d_1 d_4}]\sin(sx) + \tau_0[\frac{d_2 m_{11} e^{s\lambda_{11}(y-h)} - d_1 m_{22} e^{s\lambda_{22}(y-h)}}{d_2 d_3 - d_1 d_4}]\cos(sx)\}ds \tag{20}$$

And the stress components become:

$$\sigma_{xx}(x,y) = \frac{1}{\pi C_{66}(d_2 d_3 - d_1 d_4)}[\frac{(\sigma_0 d_3 \lambda_{22}(h-y) + \tau_0 d_1 x)(C_{11}m_{22} + C_{12}\lambda_{22})}{x^2 + (\lambda_{22}(h-y))^2} - \frac{(\sigma_0 d_4 m_{11}\lambda_{11}(h-y) + \tau_0 d_2 x)(C_{11}m_{11} + C_{12}\lambda_{11})}{x^2 + (\lambda_{11}(h-y))^2}],$$

$$\sigma_{yy}(x,y) = \frac{1}{\pi C_{66}(d_2 d_3 - d_1 d_4)}[\frac{(\sigma_0 d_3 \lambda_{22}(h-y) + \tau_0 d_1 x)(C_{12}m_{22} + C_{22}\lambda_{22})}{x^2 + (\lambda_{22}(h-y))^2} - \frac{(\sigma_0 d_4 \lambda_{11}(h-y) + \tau_0 d_2 x)(C_{12}m_{11} + C_{22}\lambda_{11})}{x^2 + (\lambda_{11}(h-y))^2}],$$

$$\sigma_{xy}(x,y) = \frac{1}{\pi(d_2 d_3 - d_1 d_4)}[\frac{(\sigma_0 d_3 x - \tau_0 d_1 \lambda_{22}(h-y))(m_{22}\lambda_{22} - 1)}{x^2 + (\lambda_{22}(h-y))^2} - \frac{(\sigma_0 d_4 x - \tau_0 d_2 \lambda_{11}(h-y))(m_{11}\lambda_{11} - 1)}{x^2 + (\lambda_{11}(h-y))^2}]. \tag{21}$$

4 Formulation of multiple moving straight cracks

Distributed dislocation technique is a method to analyze a medium containing multiple cracks. In this technique, the dislocations are distributed in the locations of the crack and the stress fields are determined for the cracked medium. Consider an orthotropic half-plane weakened by *N* moving straight cracks which can be described in parametric form as

$$\begin{aligned} &x_i = x_{i0} + a_i s, \\ &y_i = y_{i0}, \qquad -1 \le s \le 1, \quad i \in \{1,2,3,...N\}. \end{aligned} \tag{22}$$

Where (x_{i0}, y_{i0}) and a_i are the center coordinates and half-length of the *i*th crack, respectively. Suppose climb and glide edge dislocations with unknown densities $B_{yk}(t)$ and $B_{xk}(t)$, respectively, are distributed on the segment $a_k dt$ at the surface of *k*th crack, where $-1 \le t \le 1$. Covering the cracks surfaces by dislocations, the principal of superposition may be invoked to obtain traction on the crack surfaces

$$\sigma_{yy}(x_i(s),y_i(s))=\sum_{k=1}^{N}\int_{-1}^{1}[k_{yyik}^{11}(s,t)B_{xk}(t)+k_{yyik}^{12}(s,t)B_{yk}(t)]a_k dt,$$

$$\sigma_{xy}(x_i(s),y_i(s))=\sum_{k=1}^{N}\int_{-1}^{1}[k_{xyik}^{11}(s,t)B_{xk}(t)+k_{xyik}^{12}(s,t)B_{yk}(t)]a_k dt, \quad (23)$$
$$i=1,2,...,N,-1\le s\le 1.$$

The kernels k_{yyik}^{11}, k_{yyik}^{12}, k_{xyik}^{11} and k_{xyik}^{12} in integral Eqs. (24) are coefficients of b_x and b_y in stress components σ_{yy} and σ_{xy} in Eq. (18), respectively. For more details regarding the solution of singular integral equations with Cauchy type see Hills et al. [29]. The kernels in Eq. (23) exhibit Cauchy type singularity for $i=k$ as $t\to s$ and may be represented as

$$k_{yykk}^{11}(s,t)=\frac{q_{11,-1k}}{s-t}+\sum_{n=0}^{\infty}q_{11,nk}(s-t)^n,\ k_{yykk}^{12}(s,t)=\frac{q_{12,-1k}}{s-t}+\sum_{n=0}^{\infty}q_{12,nk}(s-t)^n,$$
$$k_{xykk}^{11}(s,t)=\frac{q_{21,-1k}}{s-t}+\sum_{n=0}^{\infty}q_{21,nk}(s-t)^n,k_{xykk}^{12}(s,t)=\frac{q_{22,-1k}}{s-t}+\sum_{n=0}^{\infty}q_{22,nk}(s-t)^n. \quad (24)$$

The coefficients of singular terms $q_{pm,-1k}$, $p,m=1,2$ may be obtained by means of the Taylor series expansion of $x_i(s)$ and $y_i(s)$ in the vicinity of t

$$q_{11}=S_{11}^{11}[S_{11}^{12}-S_{11}^{13}-S_{11}^{14}+S_{11}^{15}+S_{11}^{16}-S_{11}^{17}],\ q_{12}=S_{12}^{21}[S_{12}^{22}+S_{12}^{23}-S_{12}^{24}+S_{12}^{25}-S_{12}^{26}+S_{12}^{27}],$$
$$q_{21}=S_{21}^{11}[S_{21}^{12}+S_{21}^{13}-S_{21}^{14}+S_{21}^{15}+S_{21}^{16}-S_{21}^{17}],\ q_{22}=S_{22}^{21}[S_{22}^{22}+S_{22}^{23}+S_{22}^{24}+S_{22}^{25}+S_{22}^{26}+S_{22}^{27}]. \quad (25)$$

in which S_{ij}^{km}, $i,j\in\{1,2\},k\in\{1,2\},m\in\{1,2,...,7\}$ are given in Appendix C. By virtue of the Buckner's principle, Hills et al. [29], the left hand side of Eqs. (23), after changing the sign, is the traction caused by external loading on the uncracked medium at the presumed surfaces of cracks. Employing the definition of dislocation density function, the equations for the crack opening displacement across the *i*th crack yields

$$u_i(s)-u_i(s)=\int_{-1}^{s}a_i B_{xi}(t)dt,$$

$$v_i(s)-v_i(s)=\int_{-1}^{s}a_i B_{yi}(t)dt,\quad i\in\{1,2,...,N\}. \quad (26)$$

The displacement field is single valued out of an embedded crack surface. Consequently, the dislocation densities are subjected to the following closure requirements

$$\int_{-1}^{1}B_{xi}(t)dt=0,$$

$$\int_{-1}^{1}B_{yi}(t)dt=0,\quad i\in\{1,2,...,N\}. \quad (27)$$

It is worth mentioning that the devised procedure despite its simplicity is capable of handling

complicated crack arrangements. To evaluate the dislocation density, the Cauchy singular integral Eqs. (23) and Eqs. (27) ought to be solved simultaneously. The stress fields near the crack tips behave as $1/\sqrt{r}$ where r is the distance from a crack tip. Therefore, the dislocation densities are taken as

$$B_{xi}(t)=\frac{g_{xi}(t)}{\sqrt{1-t^2}},$$

$$B_{yi}(t)=\frac{g_{yi}(t)}{\sqrt{1-t^2}}, \qquad -1\le t\le 1, \qquad i\in\{1,2,...,N\}. \tag{28}$$

Substituting Eqs. (28) into Eqs. (23) and (27) as well as utilization of the numerical solutions of integral Eqs. with Cauchy-type kernel developed by Erdogan et al. [30] $g_{xi}(t)$ and $g_{yi}(t)$ can be obtained. The modes I and II stress intensity factors can be calculated based on the dislocation density functions which is derived by Fotuhi et al. [31]:

$$\begin{Bmatrix} K_{IL} \\ K_{IIL} \end{Bmatrix}=\frac{C_{66}[(\alpha_1-\alpha_4+1)\alpha_3-(\alpha_2-1)^2]}{2\alpha_3(r_1+r_2)}\left(\left[x_i'(-1)\right]^2+\left[y_i'(-1)\right]^2\right)^{\frac{1}{4}}\begin{Bmatrix} g_{ni}(-1)/r_1r_2 \\ g_{si}(-1) \end{Bmatrix},$$

$$\begin{Bmatrix} K_{IR} \\ K_{IIR} \end{Bmatrix}=-\frac{C_{66}[(\alpha_1-\alpha_4+1)\alpha_3-(\alpha_2-1)^2]}{2\alpha_3(r_1+r_2)}\left(\left[x_i'(-1)\right]^2+\left[y_i'(-1)\right]^2\right)^{\frac{1}{4}}\begin{Bmatrix} g_{ni}(1)/r_1r_2 \\ g_{si}(1) \end{Bmatrix}. \tag{29}$$

where

r_1, r_2 and H are defined

$$r_1=\sqrt{H+\sqrt{H^2-(\alpha_1-\alpha_4+1)/\alpha_3}},\ r_2=\sqrt{H-\sqrt{H^2-(\alpha_1-\alpha_4+1)/\alpha_3}},$$

$H=[(\alpha_1-\alpha_4+1)\alpha_3-\alpha_2^2+1]/2\alpha_3$, respectively. It should be mentioned subscript L and R are the left and right crack tips respectively.

5 Numerical results and discussion

Diverse numerical results will be examined to analyze the effect of velocity, material properties, multi parallel and collinear cracks as well as their lengths on the dynamic stress intensity factors. However, at first, by setting the velocity of cracks to zero, we will analyze the static crack problem in an isotropic half-plane. The stress intensity factors given by Ashbaugh [19] are compared with the present investigation. A great agreement can be observed with the above mentioned study which are given in Table (1) in which $K_0=\sigma_0\sqrt{a}$.

It is worth mentioning that the material properties used in this analysis are given in Table (2) [17]. Obviously, the only difference between orthotropic I and II is that the principle directions are perpendicular to each other. In the following examples the analysis of DSIFs for diverse crack length and diverse crack velocities are examined while the dimensionless crack velocity is considered to be $c=0.3$ and dimensionless crack length is allocated to be *a/h=1*. Also, the medium is under an equal tensile and shear moving point loads with $\sigma_0=1$ and $\tau_0=1$, and dimensionless stress intensity factors for point loads is $K_0=\sigma_0/\sqrt{a}$.

Table 1 Comparison of SIFs for a straight crack in an isotropic half-plane for right and left crack tips respectively

$\sigma_0=1$		h				
$\tau_0=0$		∞	4.0	1.0	0.4	0.1
Ashbaugh [19]	K_I/K_0	1	1.045	1.511	2.905	14.01
		1	1.045	1.511	2.905	14.01
	K_{II}/K_0	0	0.0055	0.1849	0.9940	8.812
		0	-0.0055	-0.1849	-0.9940	-8.812
Present study	K_I/K_0	1	1.0451	1.5110	2.9056	14.01
		1	1.0451	1.5510	2.9056	14.01
	K_{II}/K_0	0	0.0055	0.1849	0.9940	8.8133
		0	-0.0055	-0.1849	-0.9940	-8.8133
$\sigma_0=0$		h				
$\tau_0=1$		∞	4.0	1.0	0.4	0.1
Ashbaugh [19]	K_I/K_0	0	-0.0053	-0.1331	-0.3876	-0.8709
		0	0.0053	0.1331	0.3876	0.8709
	K_{II}/K_0	1	1.014	1.087	1.133	1.384
		1	1.014	1.087	1.133	1.384
Present study	K_I/K_0	0	-0.0053	-0.1331	-0.3876	-0.8710
		0	0.0053	0.1331	0.3876	0.8710
	K_{II}/K_0	1	1.0141	1.0873	1.1329	1.3842
		1	1.0141	1.0873	1.1329	1.3842

Table 2 Mechanical properties [17]

	$C_{11}(N/m^2)$	$C_{12}(N/m^2)$	$C_{22}(N/m^2)$	$C_{66}(N/m^2)$	$\rho(Kg/m^3)$
Isotropic	2.198×10^{11}	6.593×10^{10}	2.198×10^{11}	7.692×10^{10}	7840
Orthotropic I	1.578×10^{10}	3.248×10^{9}	1.048×10^{10}	7.070×10^{9}	1580
Orthotropic II	1.048×10^{10}	3.248×10^{9}	1.578×10^{10}	7.070×10^{9}	1580

5.1 Medium weakened by one crack propagation

In the first example, Figure (2), dynamic stress intensity factors for mode I and mode II for various material properties versus the dimensionless crack velocities is considered. It is evident that DSIFs rise gradually as long as crack velocity increases for mode I. It can be seen that DSIFs values for crack tip L are roughly one half more than the ones for crack tip R .
Also, DSIFs for orthotropic II and orthotropic I are almost quadrupled and doubled in values respectively compared to isotropic material. In stark contrast, mode II DSIFs values for isotropic material increases dramatically and DSIFs values for orthotropic II and I almost triple and double respectively as dimensionless crack velocity increases.
In the next example, a straight crack with a constant crack velocity under in plane loadings is considered. Results given in Figure (3) illustrate that by increasing the crack length, DSIFs will go up steadily. It can be seen that mode I DSIFs almost triples in value for orthotropic II as crack length increases. Moreover, according to the given diagram, crack tip L has allocated more values than the crack tip R . What is more, DSIFs for crack tips L and R .have higher and lesser values for orthotropic II and I respectively. On the other hand, mode II DSIFs shows an upward trend in which crack tip R has far more values than the other tip. Besides, mode II DSIFs have the same values for both crack tips due to symmetry in the static case; however, as crack length grows, DSIFs for crack tips diverges from each other.

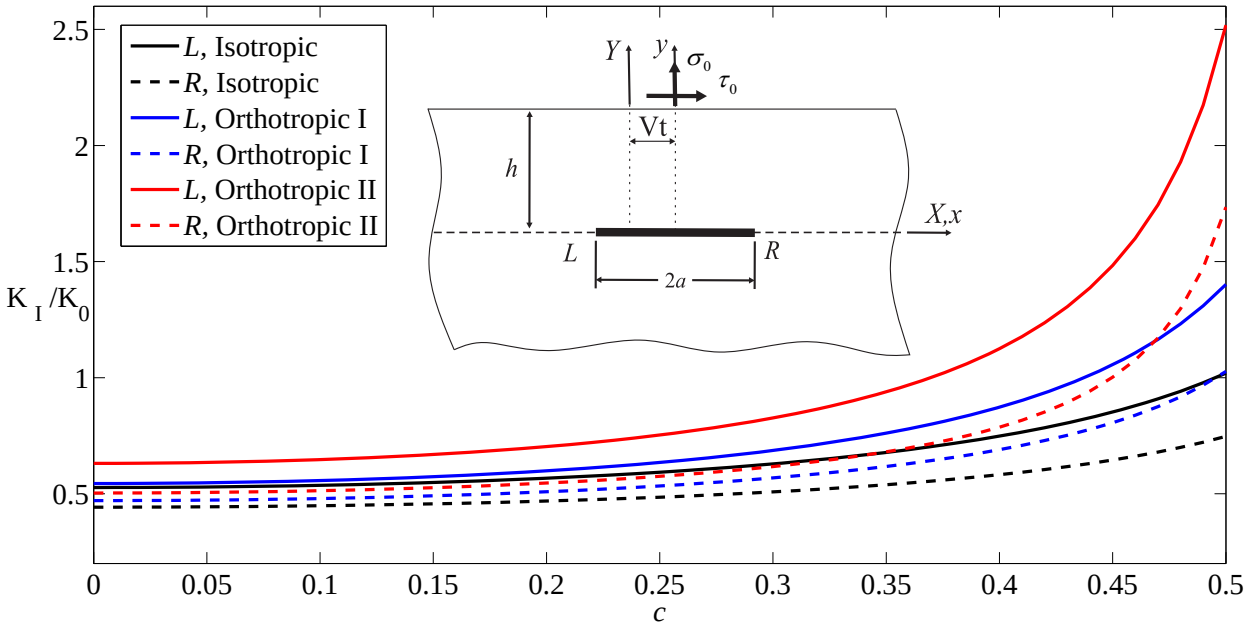

Figure 2a Mode I normalized stress intensity factors versus dimensionless crack velocity

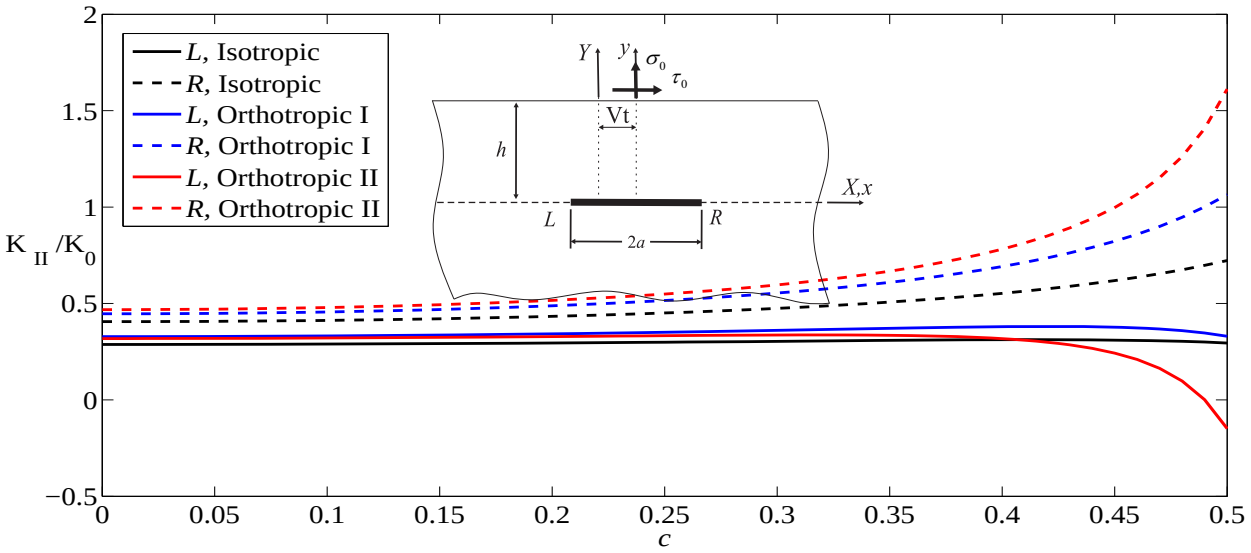

Figure 2b Mode II normalized stress intensity factors versus dimensionless crack velocity

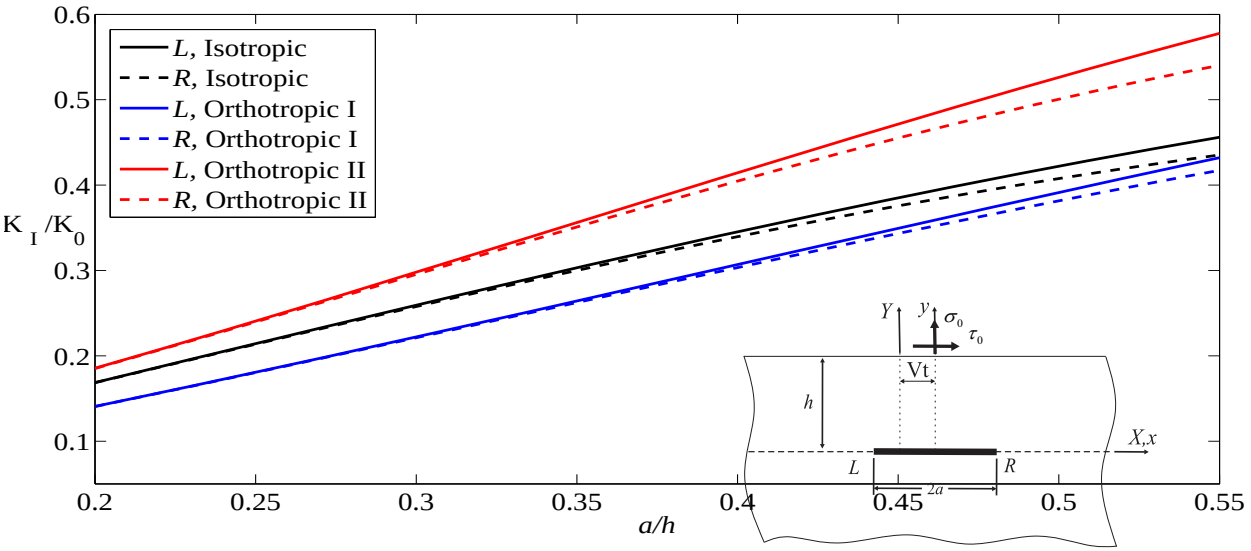

Figure 3a Mode I normalized stress intensity factors versus dimensionless crack length

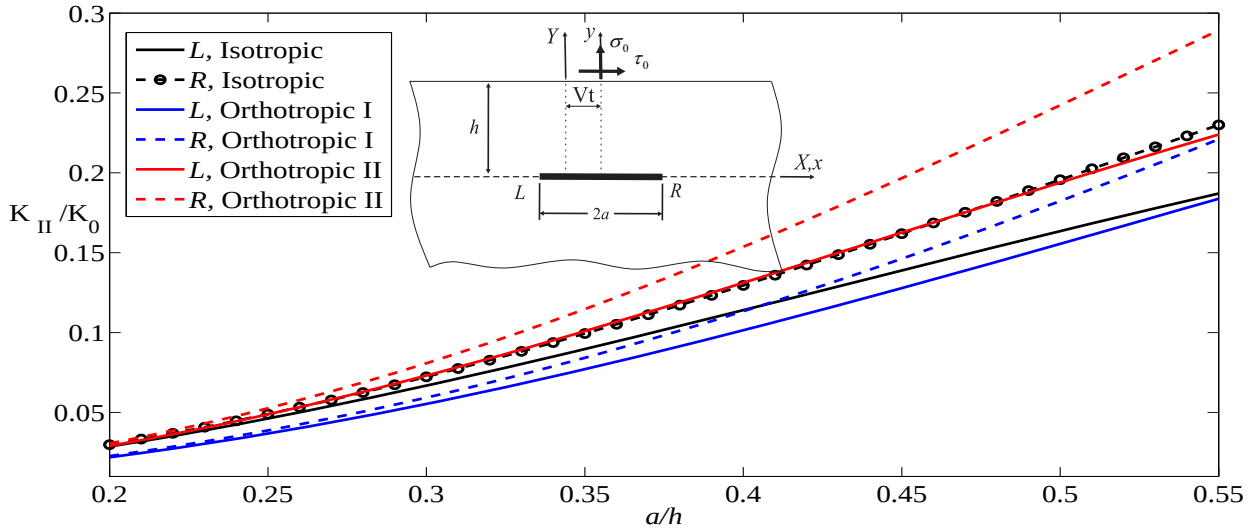

Figure 3b Mode II normalized stress intensity factors versus dimensionless crack length

5.2 Medium weakened by three parallel cracks propagation

Last but not least, three parallel cracks are taken into consideration as another example whose centers are set to have an equal distance of $0.6h$ with each other. The provided graph, Figures (4), represents contrasts between crack tips for diverse materials. It can be seen that the values of mode I DSIFs have an upward trend when crack velocity increases, especially for orthotropic II whose values almost triples as dimensionless crack velocity reaches 0.35. Besides, orthotropic I has lower values than isotropic material for each crack tips. According to the provided results, crack tips L_2, L_3, R_1 and R_2 have far more DSIFs values than the other crack tips due to their significant interaction with other cracks. It is evident that crack tips L_1 and R_3 have far less DSIFs compared to two other crack tips. On the other side, mode II DSIFs values increase considerably while crack velocity increases. It can be seen that crack tips R_2 and L_3 have by far the most DSIFs values which is due to the significant interaction between cracks. Furthermore, it is depicted that orthotropic II and I have allocated higher and lesser DSIFs values than isotropic material respectively.

Moreover, the results provided for the next example in Figures (5) presents variation of DSIFs for three parallel cracks versus crack length. According to the graphs, mode I DSIFs increase and almost quadruple as crack length doubles in value. In this case, L_3 and R_1 tips have the most values of DSIFs. Besides, DSIFs for orthotropic II has higher values than isotropic which also has more DSIFs values than orthotropic I.

The results in the provided graphs reveal that by increasing the crack lengths, interaction between cracks increases which has a significant impact on DSIFs. On the other side, the mode II DSIFs increase significantly in value while cracks lengths growth (Figures (5c) and (5d)). The DSIFs for orthotropic I and II, however, have the most variation as cracks lengths doubled. It is seen that crack tip L_2 and R_2 have the most values of DSIFs compared to other crack tips due to the considerable interaction between cracks.

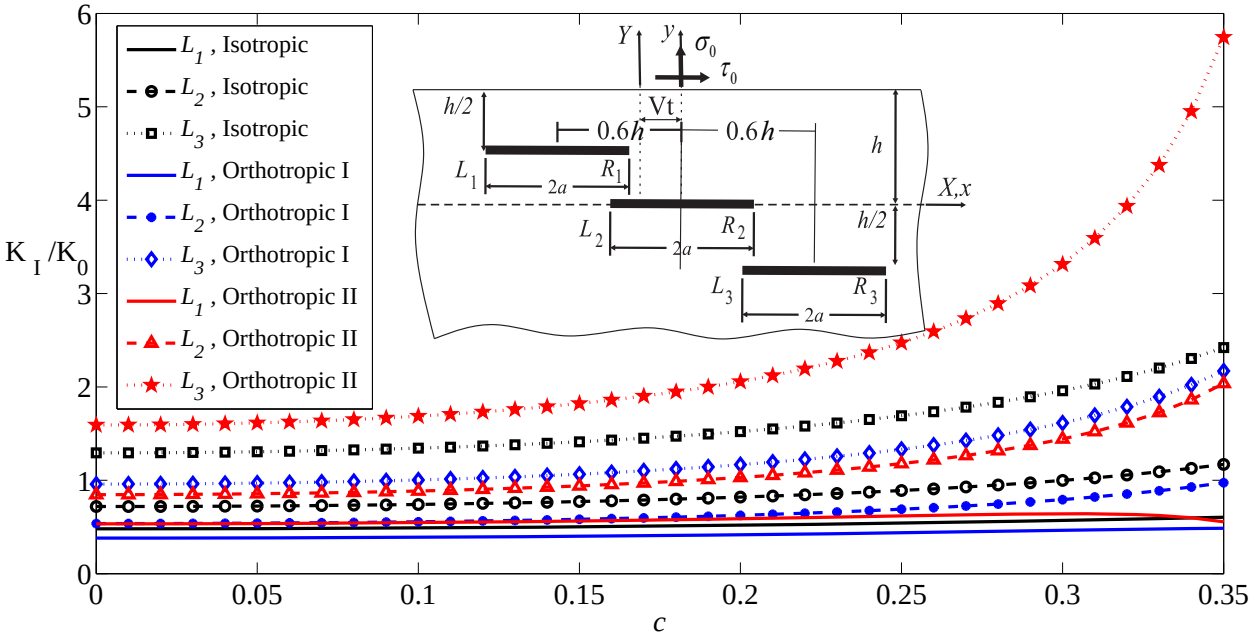

Figure 4a Variation of mode I normalized stress intensity factors of three parallel cracks with dimensionless crack velocity

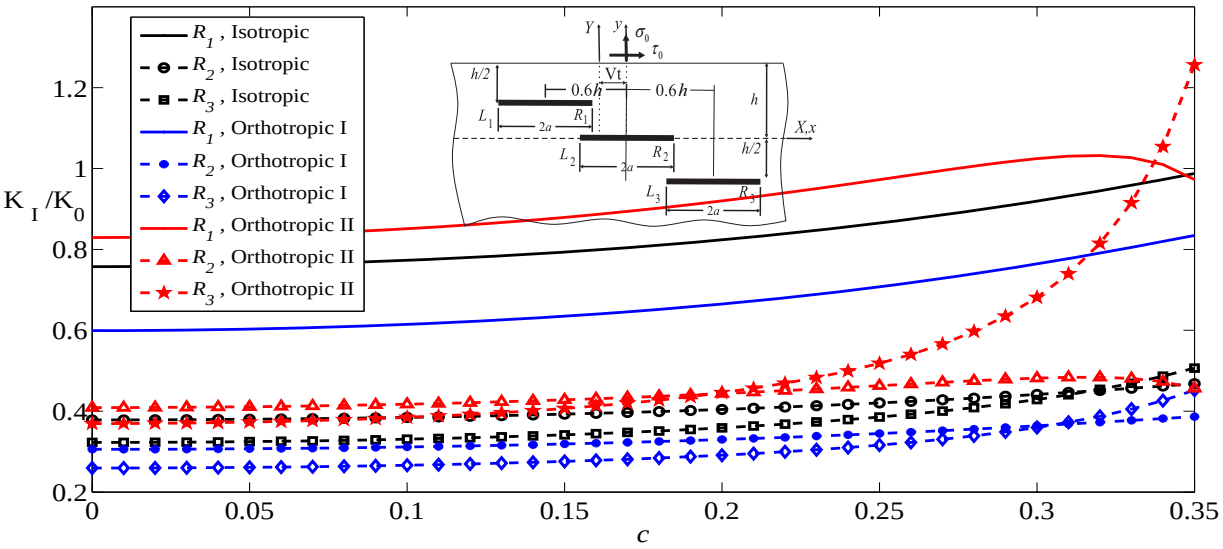

Figure 4b Variation of mode I normalized stress intensity factors of three parallel cracks with dimensionless crack velocity

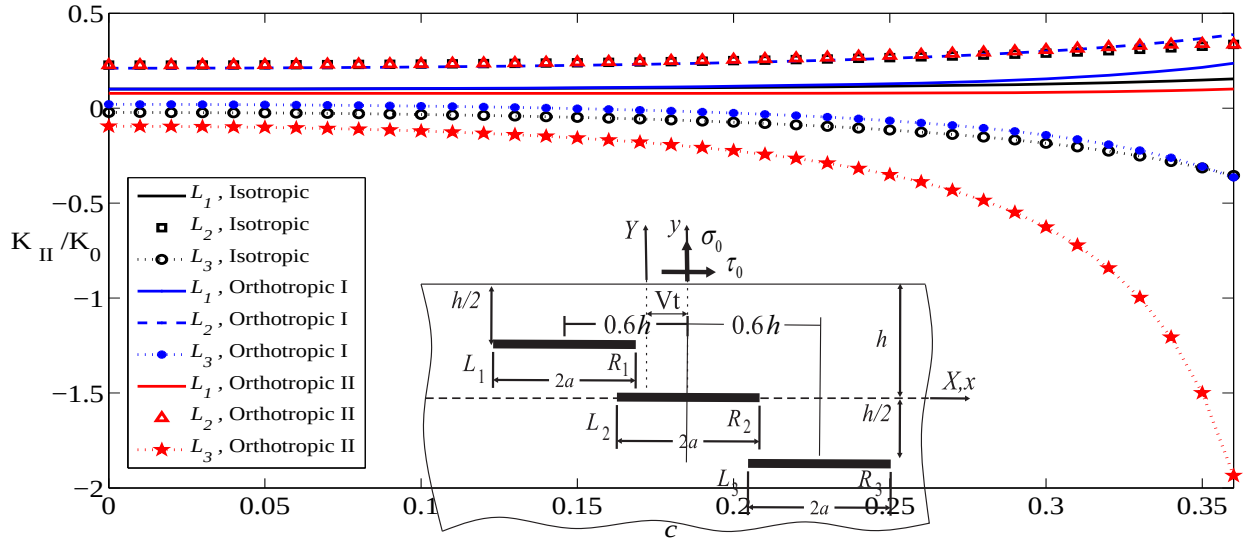

Figure 4c Variation of mode II normalized stress intensity factors of three parallel cracks with dimensionless crack velocity

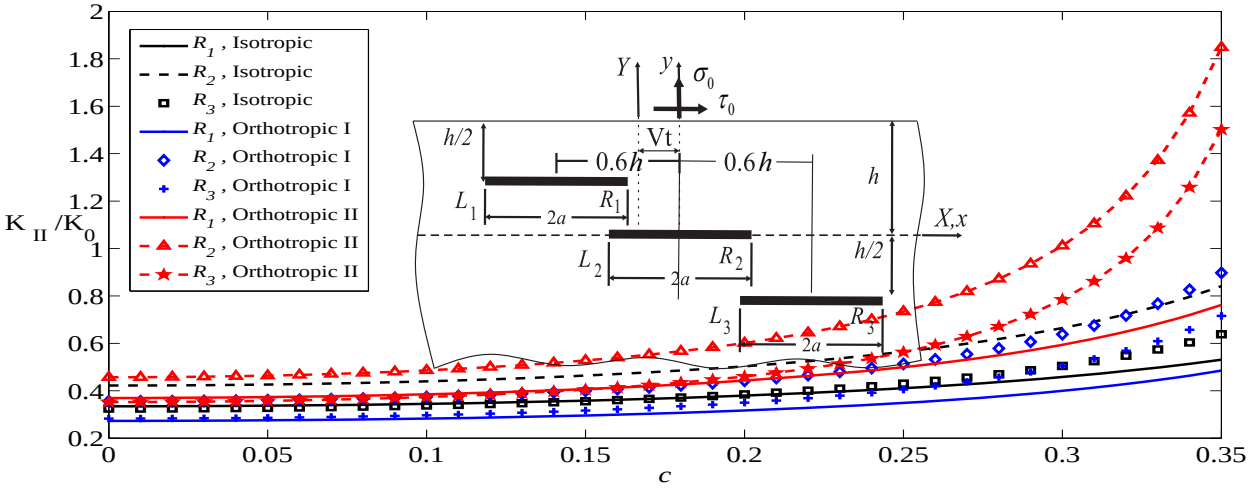

Figure 4d Variation of mode II normalized stress intensity factors of three parallel cracks with dimensionless crack velocity

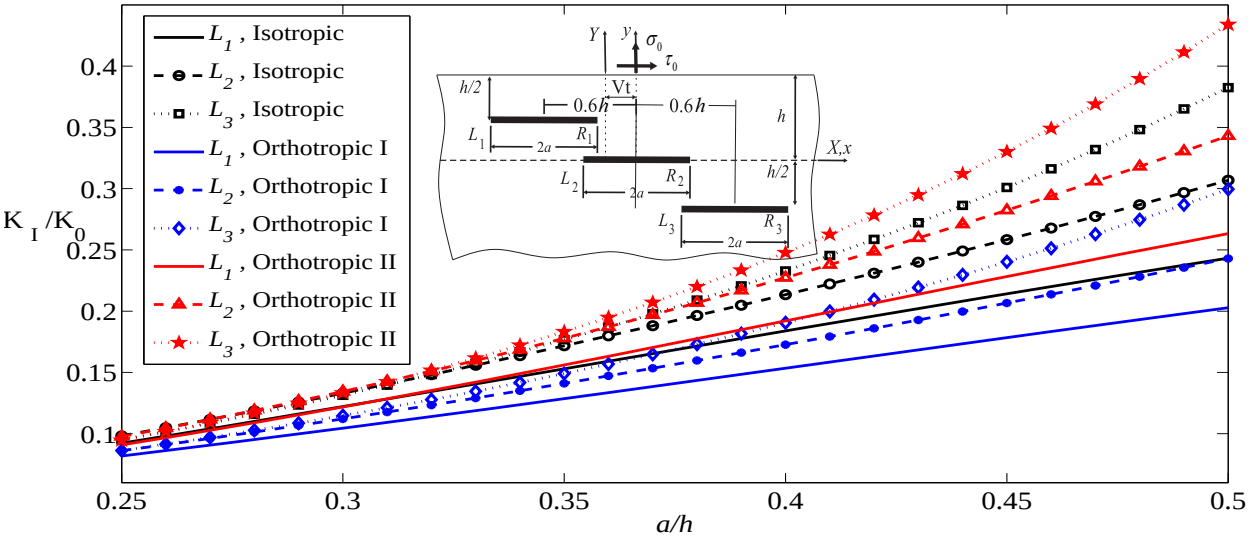

Figure 5a Variation of mode I normalized stress intensity factors of three parallel cracks with dimensionless crack length

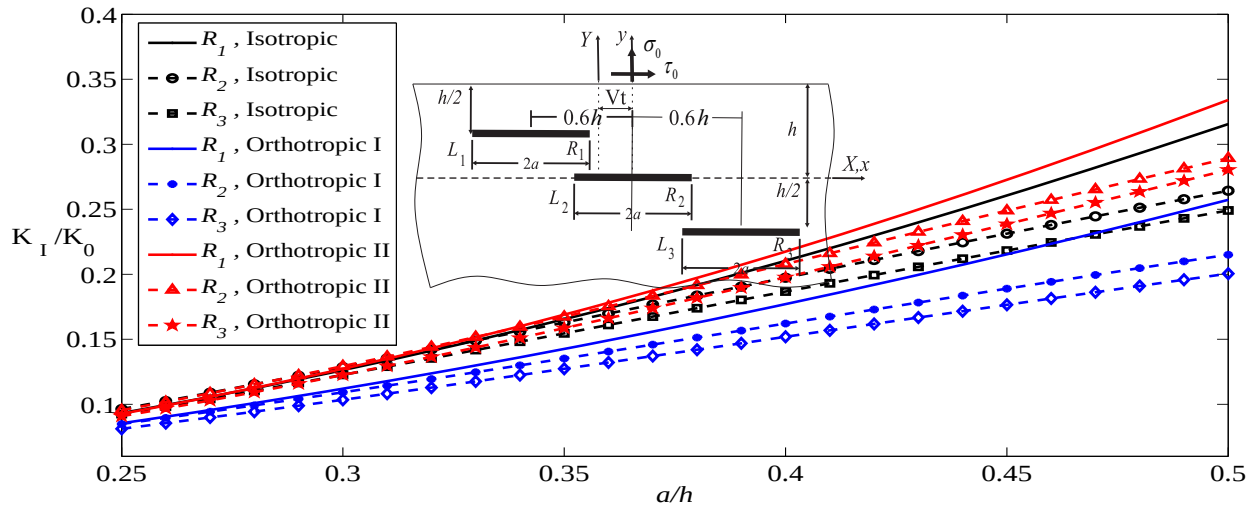

Figure 5b Variation of mode I normalized stress intensity factors of three parallel cracks with dimensionless crack length

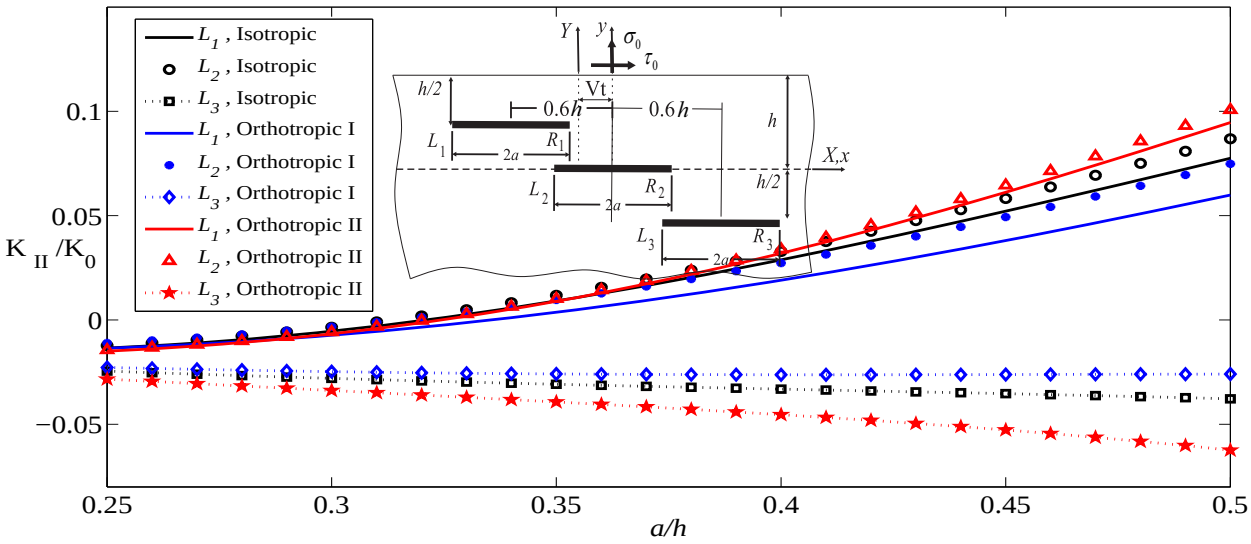

Figure 5c Variation of mode II normalized stress intensity factors of three parallel cracks with dimensionless crack length

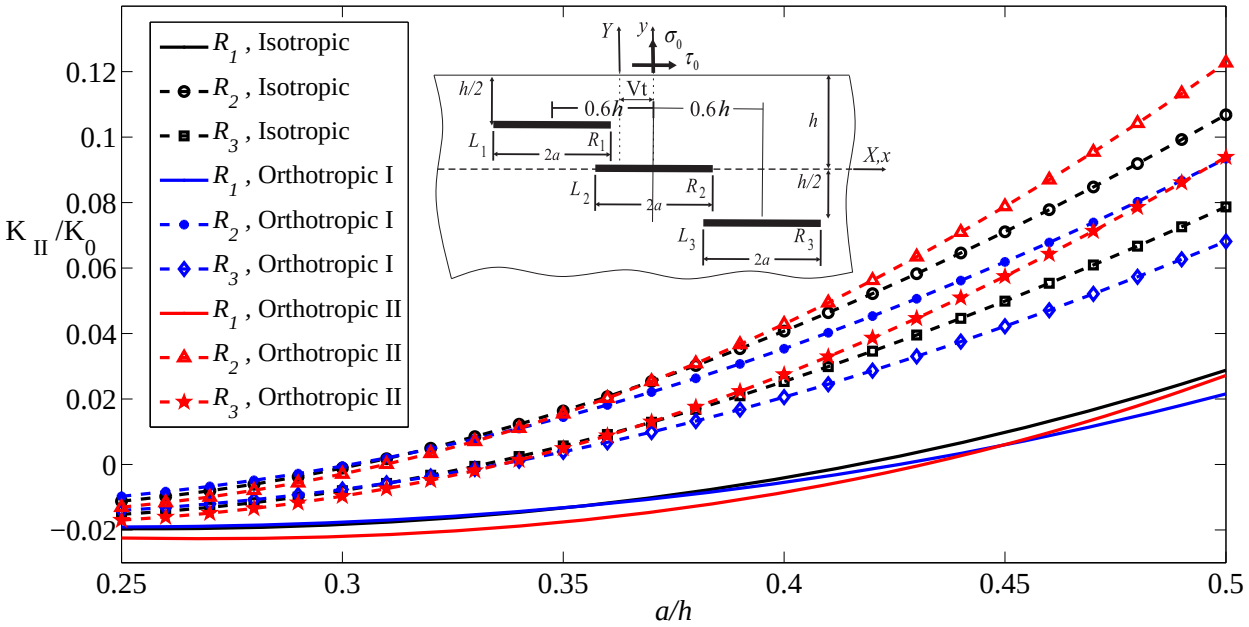

Figure 5d Variation of mode II normalized stress intensity factors of three parallel cracks with dimensionless crack length

6 Conclusion

The in-plane stress analysis of an orthotropic half-plane weakened by edge dislocations by a proper arrangement of dislocations for several cracks is analyzed. For instance, in this analysis a single and multi collinear and parallel cracks propagation are considered. The Cauchy type singularity is seen at the dislocation position for the attained stress fields. The static problem was first compared with the cited results in the literature and great agreement was observed. The effect of material properties, crack velocity, crack length, number of cracks and their arrangement on the dynamic stress intensity factors are studied.
The results illustrate that

1) The values of stress intensity factors increases so long as dimensionless crack velocity escalates.
2) By increasing the dimensionless crack the dynamic stress intensity factors increases.
3) While the normalized crack length rises, the interaction between cracks increases.
4) Materials play a significant role on the values of DSIFs. In most cases, Orthotropic II had the most DSIFs values as opposed to Orthotropic I which allocated the least amounts.

References

[1] Rubio-Gonzalez, C., and Mason, J.J., "Dynamic Stress Intensity Factors at the Tip of a Uniformly Loaded Semi-infinite Crack in an Orthotropic Material", Journal of the Mechanics and Physics of Solids, Vol. 48, pp. 899-925, (2000).

[2] Wang, C.Y., Rubio-Gonzalez, C., and Mason, J.J., "The Dynamic Stress Intensity Factor for a Semi-infinite Crack in Orthotropic Materials with Concentrated Shear Impact Loads", International Journal of Solids and Structures, Vol. 38, pp. 1265-1280, (2001).

[3] Li, X.F., and Guo, S.H., "Effects of Nonhomogeneity on Dynamic Stress Intensity Factors for an Antiplane Interface Crack in a Functionally Graded Material Bonded to an Elastic Semi-strip", Computational Materials Science, Vol. 38, pp. 432-441, (2006).

[4] Itou, S., "Dynamic Stress Intensity Factors around a Cylindrical Crack in an Infinite Elastic Medium Subject to Impact Load", International Journal of Solids and Structures, Vol. 44, pp. 7340-7356, (2007).

[5] Itou, S., "Dynamic Stress Intensity Factors for Two Parallel Interface Cracks Between a Nonhomogeneous Bonding Layer and Two Dissimilar Elastic Half-planes Subject to an Impact Load", International Journal of Solids and Structures, Vol. 47, pp. 2155-2163, (2010).

[6] Xu, H., Yao, X., Feng, X., and Hisen, Y. Y., "Dynamic Stress Intensity Factors of a Semi-infinite Crack in an Orthotropic Functionally Graded Material", Mechanics of Materials, Vol. 40, pp. 37-47, (2008).

[7] Zhao, W., Hu, Z., Zhang, X., Xie, H., and Yu, L., "The Dynamic Stress Intensity Factor Around the Anti-plane Crack in an Infinite Strip Functionally Graded Material under Impact Loading", Theoretical and Applied Fracture Mechanics, Vol. 74, pp. 1-6, (2014).

[8] Rubio-Gonzalez, C., and Mason, J. J., "Mixed Mode Dynamic Stress Intensity Factor Due to applied point loads", Computers & Structures, Vol. 76, pp. 237-245, (2000).

[9] Rubio-Gonzalez, C., and Mason, J. J., "Dynamic Stress Intensity Factor for a Propagating Semi-infinite Crack in Orthotropic Materials", International Journal of Engineering Science, Vol. 39, pp. 15-38, (2001).

[10] Ma, C. C., and Chen, S. K., "Dynamic Stress Intensity Factor for Subsurface Inclined Cracks", Journal of Engineering Mechanics, Vol. 120, pp. 483-498, (1994).

[11] Jin, B., and Zhong, Z., "Dynamic Stress Intensity Factor (Mode I) of a Penny-shaped Crack in an Infinite Poroelastic Solid", International Journal of Engineering Science, Vol. 40, pp. 637-646, (2002).

[12] Zhang, C., Sladek, J., and Sladek, V., "Effects of Material Gradients on Transient Dynamic Mode-III Stress Intensity Factors in a FGM", International Journal of Solids and Structures, Vol. 40, pp. 5251-5270, (2003).

[13] Itou, S., "Transient Dynamic Stress Intensity Factors around Three Stacked Parallel Cracks in an Infinite Medium during Passage of an Impact Normal Stress", International Journal of Solids and Structures, Vol. 78–79, pp. 199-204, (2016).

[14] Antipov, Y.A., and Smirnov, A.V., "Fundamental Solution and the Weight Functions of the Transient Problem on a Semi-infinite Crack Propagating in a Half-plane", ZAMM - Journal of Applied Mathematics and Mechanics, Vol. 96, pp. 1156-1174, (2016).

[15] Ma, L., Wu, L.Z., Zhou, Z. G., and Zeng, T., "Crack Propagating in a Functionally Graded Strip under the Plane Loading", International Journal of Fracture, Vol. 126, pp. 39-55, (2004).

[16] Ma, L., Wu, L.z., and Guo, L.C., "On the Moving Griffith Crack in a Nonhomogeneous Orthotropic Strip", International Journal of Fracture, Vol. 136, pp. 187-205, (2005).

[17] Ma, L., Wu, L.Z., Guo, L.C., and Zhou, Z. G., "On the Moving Griffith Crack in a Non-homogeneous Orthotropic Medium", European Journal of Mechanics A/Solids, Vol. 24, pp. 393-405, (2005).

[18] Song, S. H., and Paulino, G. H., "Dynamic Stress Intensity Factors for Homogeneous and Smoothly Heterogeneous Materials using the Interaction Integral Method", International Journal of Solids and Structures, Vol. 43, pp. 4830-4866, (2006).

[19] Ashbaugh, N., "Stress Solution for a Crack at an Arbitrary Angle to an Interface", International Journal of Fracture, Vol. 11, pp. 205-219, (1975).

[20] Aijun, C., "Study on Dynamic Stress Intensity Factors of Disk with a Radial Edge Crack Subjected to External Impulsive Pressure", Acta Mechanica Solida Sinica, Vol. 20, pp. 41-49, (2007).

[21] Malekzadeh Fard, K., Monfared, M.M., and Norouzipour, K., "Determination of Stress Intensity Factors in Half-plane Containing Several Moving Cracks", Applied Mathematics and Mechanics, Vol. 34, pp. 1535-1542, (2013).

[22] Wang, Z., Ma, L., Yu, H., and Wu, L., "Dynamic Stress Intensity Factors for Homogeneous and Non-homogeneous Materials using the Interaction Integral Method", Engineering Fracture Mechanics, Vol. 128, pp. 8-21, (2014).

[23] Ma, L., Li, J., Abdelmoula, R., and Wu, L. Z., "Dynamic Stress Intensity Factor for Cracked Functionally Graded Orthotropic Medium under Time-harmonic Loading", European Journal of Mechanics A/Solids, Vol. 26, pp. 325-336, (2007).

[24] Monfared, M. M., and Ayatollahi, M., "Dynamic Stress Intensity Factors of Multiple Cracks in a Functionally Graded Orthotropic Half-plane", Theoretical and Applied Fracture Mechanics, Vol. 56, pp. 49-57, (2011).

[25] Monfared, M. M., and Ayatollahi, M., "Dynamic Stress Intensity Factors of Multiple Cracks in an Orthotropic Strip with FGM Coating", Engineering Fracture Mechanics, Vol. 109, pp. 45-57, (2013).

[26] Itou, S., "Effect of Couple-stresses on the Mode I Dynamic Stress Intensity Factors for Two Equal Collinear Cracks in an Infinite Elastic Medium during Passage of Time-harmonic Stress Waves", International Journal of Solids and Structures, Vol. 50, pp. 1597-1604, (2013).

[27] Itou, S., "Effect of Couple-stresses on the Stress Intensity Factors for a Crack in an Infinite Elastic Strip under Tension", European Journal of Mechanics A/Solids, Vol. 42, pp. 335-343, (2013).

[28] Itou, S., "Dynamic Stress Intensity Factors of Three Collinear Cracks in an Orthotropic Plate Subjected to Time-harmonic Disturbance", Journal of Mechanics, Vol. 32, pp. 491-499, (2016).

[29] Hills, D.A., K. P. A., Dai, D.N., and Korsunsky, A.M., "Solution of Crack Problems:The Distributed Dislocation Technique", Kluwer Academic Publishers, (1996).

[30] Erdogan, F., Gupta, G. D., and Cook, T. S., "Numerical Solution of Singular Integral Equations, in Methods of Analysis and Solutions of Crack Problems: Recent Developments in Fracture Mechanics Theory and Methods of Solving Crack Problems", Sih, G. C., Editor., Springer Netherlands: Dordrecht. pp. 368-425, (1973).

[31] Fotuhi, A. R., Faal, R. T., and Fariborz, S. J., "In-plane Analysis of a Cracked Orthotropic Half-plane", International Journal of Solids and Structures, Vol. 44, pp. 1608-1627, (2007).

Appendix

Appendix A:

$$B_1(s)=\frac{(\pi\delta(s)+i/s)}{2}\left(\frac{i\,\mathrm{sgn}(s)d_2b_x}{d_2m_{11}-d_1m_{22}}-\frac{d_4b_y}{d_3-d_4}\right),\quad B_2(s)=\frac{(\pi\delta(s)+i/s)}{2}\left(\frac{d_3b_y}{d_3-d_4}+\frac{i\,\mathrm{sgn}(s)d_1b_x}{d_1m_{22}-d_2m_{11}}\right),$$

$$B_3(s)=\frac{(\pi\delta(s)+i/s)}{2(d_2d_3-d_1d_4)}\left[\frac{(2d_1d_4e^{-h|s|(\lambda_{11}+\lambda_{22})}-(d_2d_3+d_1d_4)e^{-2h|s|\lambda_{11}})d_2i\,\mathrm{sgn}(s)b_x}{d_2m_{11}-d_1m_{22}}\right.$$
$$\left.+\frac{((d_2d_3+d_1d_4)e^{-2h|s|2\lambda_{11}}-2d_2d_3e^{-h|s|(\lambda_{11}+\lambda_{22})})d_4b_y}{d_3-d_4}\right],$$

$$B_4(s)=\frac{(\pi\delta(s)+i/s)}{2(d_2d_3-d_1d_4)}\left[\frac{(2d_2d_3e^{-h|s|(\lambda_{11}+\lambda_{22})}-(d_2d_3+d_1d_4)e^{-2h|s|\lambda_{22}})id_1\,\mathrm{sgn}(s)b_x}{d_2m_{11}-d_1m_{22}}\right.$$
$$\left.+\frac{((d_2d_3+d_1d_4)e^{-2h|s|\lambda_{22}}-2d_1d_4e^{-h|s|(\lambda_{11}+\lambda_{22})})d_3b_y}{d_3-d_4}\right],$$

$$B_5(s)=\frac{(\pi\delta(s)+i/s)}{2(d_2d_3-d_1d_4)}\left[\frac{((2e^{-h|s|(\lambda_{11}+\lambda_{22})}-e^{-2h|s|\lambda_{11}}-1)d_1d_4+(1-e^{-2h|s|\lambda_{11}})d_2d_3)id_2\,\mathrm{sgn}(s)b_x}{d_2m_{11}-d_1m_{22}}\right.$$
$$\left.+\frac{((-2e^{-h|s|(\lambda_{11}+\lambda_{22})}+e^{-2h|s|\lambda_{11}}+1)d_2d_3-(1-e^{2h|s|\lambda_{11}})d_1d_4)d_4b_y}{d_3-d_4}\right],$$

$$B_6(s)=\frac{(\pi\delta(s)+i/s)}{2(d_2d_3-d_1d_4)}\left[\frac{((-e^{-2h|s|\lambda_{22}}+2e^{-h|s|(\lambda_{11}+\lambda_{22})}-1)d_2d_3+(1-e^{-2h|s|\lambda_{22}})d_1d_4)i\,\mathrm{sgn}(s)d_1b_x}{d_2m_{11}-d_1m_{22}}\right.$$
$$\left.+\frac{((e^{-2h|s|\lambda_{22}}-2e^{-h|s|(\lambda_{11}+\lambda_{22})}+1)d_1d_4+(-1+e^{-2h|s|\lambda_{22}})d_2d_3)d_3b_y}{d_3-d_4}\right].$$

(A1)

Appendix B:

$$T_u^{11}=\frac{1}{2s(d_2m_{11}-d_1m_{22})(d_2d_3-d_1d_4)},T_u^{12}=(d_2d_3-d_1d_4)(d_2m_{11}e^{-sy\lambda_{11}}-d_1m_{22}e^{-sy\lambda_{22}})$$
$$T_u^{13}=d_1d_2d_4m_{11}(e^{s(-2h+y)\lambda_{11}}-2e^{-s((h-y)\lambda_{11}+h\lambda_{22})}),T_u^{14}=d_1d_2d_3m_{22}(e^{s(-2h+y)\lambda_{22}}-2e^{-s(h\lambda_{11}+(h-y)\lambda_{22})})$$
$$T_u^{15}=d_1^2d_4m_{22}e^{s(-2h+y)\lambda_{22}}+d_2^2d_3m_{11}e^{s(-2h+y)\lambda_{11}}$$

$$T_u^{21}=\frac{1}{2s(d_3-d_4)(d_2d_3-d_1d_4)},T_u^{22}=(d_2d_3-d_1d_4)(d_3m_{22}e^{-sy\lambda_{22}}-d_4m_{11}e^{-sy\lambda_{11}})$$
$$T_u^{23}=d_2d_3d_4m_{11}(2e^{-s((h-y)\lambda_{11}+h\lambda_{22})}-e^{s(-2h+y)\lambda_{11}}),T_u^{24}=-(d_1d_4^2m_{11}e^{s(-2h+y)\lambda_{11}}+d_2d_3^2m_{22}e^{s(-2h+y)\lambda_{22}})$$
$$T_u^{25}=d_1d_3d_4m_{22}(2e^{-s(h\lambda_{11}+(h-y)\lambda_{22})}-e^{s(-2h+y)\lambda_{22}})$$

(B1)

$$T_v^{11}=\frac{1}{2s(d_2m_{11}-d_1m_{22})(d_2d_3-d_1d_4)},T_v^{12}=(d_2d_3-d_1d_4)(d_1e^{-sy\lambda_{22}}-d_2e^{-sy\lambda_{11}})$$
$$T_v^{13}=d_1d_2d_3(e^{s(-2h+y)\lambda_{22}}-2e^{-s(h\lambda_{11}+(h-y)\lambda_{22})}),T_v^{14}=d_2^2d_3e^{s(-2h+y)\lambda_{11}}+d_1^2d_4e^{s(-2h+y)\lambda_{22}}$$
$$T_v^{15}=d_1d_2d_4(e^{s(-2h+y)\lambda_{11}}-2e^{-s((h-y)\lambda_{11}+h\lambda_{22})}).$$

(B2)

$$T_v^{21}=\frac{1}{2s(d_3-d_4)(d_2d_3-d_1d_4)},T_v^{22}=d_2d_3^2(\mathrm{e}^{-sy\lambda_{22}}+\mathrm{e}^{s(-2h+y)\lambda_{22}})$$
$$T_v^{23}=d_1d_3d_4(\mathrm{e}^{s(-2h+y)\lambda_{22}}-\mathrm{e}^{-sy\lambda_{22}}-2\mathrm{e}^{-s(h\lambda_{11}+(h-y)\lambda_{22})}),$$
$$T_v^{24}=d_2d_3d_4(\mathrm{e}^{s(-2h+y)\lambda_{11}}-2\mathrm{e}^{-s((h-y)\lambda_{11}+h\lambda_{22})}-\mathrm{e}^{-sy\lambda_{11}}),T_v^{25}=d_1d_4^2(\mathrm{e}^{-sy\lambda_{11}}+\mathrm{e}^{s(-2h+y)\lambda_{11}}).$$

(B3)

Appendix C:

$$S_{xx}^{11}=\frac{C_{66}}{2\pi(d_2m_{11}-d_1m_{22})(d_2d_3-d_1d_4)}$$
$$S_{xx}^{12}=\frac{m_{11}\lambda_{11}y(\alpha_1-\alpha_4+1)(d_2^2d_3-d_1d_2d_4)+\lambda_{11}^2y(\alpha_2-1)(d_2^2d_3-d_1d_2d_4)}{x^2+(\lambda_{11}y)^2}$$
$$S_{xx}^{13}=\frac{m_{22}\lambda_{22}y(\alpha_1-\alpha_4+1)(d_1d_2d_3-d_1^2d_4)+\lambda_{22}^2y(\alpha_2-1)(d_1d_2d_3-d_1^2d_4)}{x^2+(\lambda_{22}y)^2}$$
$$S_{xx}^{14}=\frac{2d_1d_2d_4(\lambda_{11}h+\lambda_{22}h-\lambda_{11}y)[(\alpha_1-\alpha_4+1)m_{11}+(\alpha_2-1)\lambda_{11}]}{x^2+(\lambda_{11}h+\lambda_{22}h-\lambda_{11}y)^2}$$
$$S_{xx}^{15}=\frac{(d_2d_3+d_1d_4)(2\lambda_{11}h-\lambda_{11}y)[(\alpha_1-\alpha_4+1)d_2m_{11}+(\alpha_2-1)d_2\lambda_{11}]}{x^2+(2\lambda_{11}h-\lambda_{11}y)^2}$$

$$S_{xx}^{16}=\frac{(d_2d_3+d_1d_4)(2\lambda_{22}h-\lambda_{22}y)[(\alpha_1-\alpha_4+1)d_1m_{22}+(\alpha_2-1)d_1\lambda_{22}]}{x^2+(2\lambda_{22}h-\lambda_{22}y)^2}$$

$$S_{xx}^{17}=\frac{2d_1d_2d_3(\lambda_{11}h+\lambda_{22}h-\lambda_{22}y)[(\alpha_1-\alpha_4+1)m_{22}+(\alpha_2-1)\lambda_{22}]}{x^2+(\lambda_{11}h+\lambda_{22}h-\lambda_{22}y)^2}$$

$$S_{xx}^{21}=\frac{xC_{66}}{2\pi(d_2d_3-d_1d_4)(d_3-d_4)},S_{xx}^{22}=\frac{(-d_1d_4^2+d_2d_3d_4)[(\alpha_1-\alpha_4+1)m_{11}+(\alpha_2-1)\lambda_{11}]}{x^2+(\lambda_{11}y)^2}$$

$$S_{xx}^{23}=\frac{(-d_2d_3^2+d_1d_3d_4)[(\alpha_1-\alpha_4+1)m_{22}+(\alpha_2-1)\lambda_{22}]}{x^2+(\lambda_{22}y)^2}$$

$$S_{xx}^{24}=\frac{2d_2d_3d_4[(\alpha_1-\alpha_4+1)m_{11}+(\alpha_2-1)\lambda_{11}]}{x^2+(\lambda_{11}h+\lambda_{22}h-\lambda_{11}y)^2}$$

$$S_{xx}^{25}=\frac{(d_2d_3+d_1d_4)[(\alpha_1-\alpha_4+1)d_4m_{11}+(\alpha_2-1)d_4\lambda_{11}]}{x^2+(2\lambda_{11}h-\lambda_{11}y)^2}$$

$$S_{xx}^{26}=\frac{2d_1d_4d_3[(\alpha_1-\alpha_4+1)m_{22}+(\alpha_2-1)\lambda_{22}]}{x^2+(\lambda_{11}h+\lambda_{22}h-\lambda_{22}y)^2}$$

$$S_{xx}^{27}=\frac{(d_2d_3+d_1d_4)[(\alpha_1-\alpha_4+1)d_3m_{22}+(\alpha_2-1)d_3\lambda_{22}]}{x^2+(2\lambda_{22}h-\lambda_{22}y)^2}$$

(C1)

$$S_{yy}^{11}=\frac{C_{66}}{2\pi(d_2m_{11}-d_1m_{22})(d_2d_3-d_1d_4)}$$

$$S_{yy}^{12}=\frac{(m_{11}\lambda_{11}y(\alpha_2-1)+\alpha_3\lambda_{11}^2y)(d_2^2d_3-d_1d_2d_4)}{x^2+(\lambda_{11}y)^2}$$

$$S_{yy}^{13}=\frac{(m_{22}\lambda_{22}y(\alpha_2-1)+\alpha_3\lambda_{22}^2y)(d_1d_2d_3-d_1^2d_4)}{x^2+(\lambda_{22}y)^2},$$

$$S_{yy}^{14}=\frac{2d_1d_2d_4(\lambda_{11}h+\lambda_{22}h-\lambda_{11}y)[(\alpha_2-1)m_{11}+\alpha_3\lambda_{11}]}{x^2+(\lambda_{11}h+\lambda_{22}h-\lambda_{11}y)^2}$$

$$S_{yy}^{15}=\frac{(d_2d_3+d_1d_4)(2\lambda_{11}h-\lambda_{11}y)[(\alpha_2-1)d_2m_{11}+\alpha_3d_2\lambda_{11}]}{x^2+(2\lambda_{11}h-\lambda_{11}y)^2}$$

$$S_{yy}^{16}=\frac{(d_2d_3+d_1d_4)(2\lambda_{22}h-\lambda_{22}y)[(\alpha_2-1)d_1m_{22}+\alpha_3d_1\lambda_{22}]}{x^2+(2\lambda_{22}h-\lambda_{22}y)^2}$$

$$S_{yy}^{17}=\frac{2d_1d_2d_3(\lambda_{11}h+\lambda_{22}h-\lambda_{22}y)[(\alpha_2-1)m_{22}+\alpha_3\lambda_{22}]}{x^2+(\lambda_{11}h+\lambda_{22}h-\lambda_{22}y)^2}$$

$$S_{yy}^{21}=\frac{xC_{66}}{2\pi(d_2d_3-d_1d_4)(d_3-d_4)},\ S_{yy}^{22}=\frac{(-d_1d_4^2+d_2d_3d_4)[(\alpha_2-1)m_{11}+\alpha_3\lambda_{11}]}{x^2+(\lambda_{11}y)^2}$$
$$S_{yy}^{23}=\frac{(-d_2d_3^2+d_1d_3d_4)[(\alpha_2-1)m_{22}+\alpha_3\lambda_{22}]}{x^2+(\lambda_{22}y)^2},\ S_{yy}^{24}=\frac{2d_2d_3d_4[(\alpha_2-1)m_{11}+\alpha_3\lambda_{11}]}{x^2+(\lambda_{11}h+\lambda_{22}h-\lambda_{11}y)^2}$$
$$S_{yy}^{25}=\frac{(d_2d_3+d_1d_4)[(\alpha_2-1)d_4m_{11}+\alpha_3d_4\lambda_{11}]}{x^2+(2\lambda_{11}h-\lambda_{11}y)^2},\ S_{yy}^{26}=\frac{2d_1d_4d_3[(\alpha_2-1)m_{22}+\alpha_3\lambda_{22}]}{x^2+(\lambda_{11}h+\lambda_{22}h-\lambda_{22}y)^2}$$
$$S_{yy}^{27}=\frac{(d_2d_3+d_1d_4)[(\alpha_2-1)d_3m_{22}+\alpha_3d_3\lambda_{22}]}{x^2+(2\lambda_{22}h-\lambda_{22}y)^2}.$$

(C2)

$$S_{xy}^{11}=\frac{xC_{66}}{2\pi(d_2m_{11}-d_1m_{22})(d_2d_3-d_1d_4)},S_{xy}^{12}=\frac{(m_{11}\lambda_{11}-1)(d_1d_2d_4-d_2^2d_3)}{x^2+(\lambda_{11}y)^2}$$
$$S_{xy}^{13}=\frac{(m_{22}\lambda_{22}-1)(d_1d_2d_3-d_1^2d_4)}{x^2+(\lambda_{22}y)^2},\ S_{xy}^{14}=\frac{2d_1d_2d_4(m_{11}\lambda_{11}-1)}{x^2+(\lambda_{11}h+\lambda_{22}h-\lambda_{11}y)^2},$$
$$S_{xy}^{15}=\frac{(d_2^2d_3+d_1d_2d_4)(m_{11}\lambda_{11}-1)}{x^2+(2\lambda_{11}h-\lambda_{11}y)^2},\ S_{xy}^{16}=\frac{(d_1d_2d_3+d_1^2d_4)(m_{22}\lambda_{22}-1)}{x^2+(2\lambda_{22}h-\lambda_{22}y)^2},$$
$$S_{xy}^{17}=\frac{2d_1d_2d_3(m_{22}\lambda_{22}-1)}{x^2+(\lambda_{11}h+\lambda_{22}h-\lambda_{22}y)^2}.$$

$$S_{xy}^{21}=\frac{C_{66}}{2\pi(d_2d_3-d_1d_4)(d_4-d_3)},\ S_{xy}^{22}=\frac{y\lambda_{11}(m_{11}\lambda_{11}-1)(-d_2d_3d_4+d_1d_4^2)}{x^2+(\lambda_{11}y)^2}$$
$$S_{xy}^{23}=\frac{y\lambda_{22}(m_{22}\lambda_{22}-1)(-d_1d_3d_4+d_2d_3^2)}{x^2+(\lambda_{22}y)^2},\ S_{xy}^{24}=\frac{2d_2d_3d_4(\lambda_{11}h+\lambda_{22}h-\lambda_{11}y)(1-m_{11}\lambda_{11})}{x^2+(\lambda_{11}h+\lambda_{22}h-\lambda_{11}y)^2}$$
$$S_{xy}^{25}=\frac{(d_2d_3d_4+d_1d_4^2)(2\lambda_{11}h-\lambda_{11}y)(-1+m_{11}\lambda_{11})}{x^2+(2\lambda_{11}h-\lambda_{11}y)^2},\ S_{xy}^{26}=\frac{2d_1d_3d_4(\lambda_{11}h+\lambda_{22}h-\lambda_{22}y)(1-m_{22}\lambda_{22})}{x^2+(\lambda_{11}h+\lambda_{22}h-\lambda_{22}y)^2}$$
$$S_{xy}^{27}=\frac{(d_2d_3^2+d_1d_3d_4)(2\lambda_{22}h-\lambda_{22}y)(-1+m_{22}\lambda_{22})}{x^2+(2\lambda_{22}h-\lambda_{22}y)^2}.$$

(C3)

$$S_{11}^{11}=\frac{C_{66}}{2\pi(d_2m_{11}-d_1m_{22})(d_2d_3-d_1d_4)},S_{yy}^{12}=0,S_{yy}^{13}=0,$$
$$S_{11}^{14}=\frac{2d_1d_2d_4(\lambda_{11}h+\lambda_{22}h)[(\alpha_2-1)m_{11}+\alpha_3\lambda_{11}]}{a_k^2+(\lambda_{11}h+\lambda_{22}h)^2},S_{11}^{15}=\frac{2\lambda_{11}h(d_2d_3+d_1d_4)[(\alpha_2-1)d_2m_{11}+\alpha_3d_2\lambda_{11}]}{a_k^2+(2\lambda_{11}h)^2},$$
$$S_{11}^{16}=\frac{2\lambda_{22}h(d_2d_3+d_1d_4)[(\alpha_2-1)d_1m_{22}+\alpha_3d_1\lambda_{22}]}{a_k^2+(2\lambda_{22}h)^2},S_{11}^{17}=\frac{2d_1d_2d_3(\lambda_{11}h+\lambda_{22}h)[(\alpha_2-1)m_{22}+\alpha_3\lambda_{22}]}{a_k^2+(\lambda_{11}h+\lambda_{22}h)^2}.$$

(C4)

$$S_{12}^{21}=\frac{a_k C_{66}}{2\pi(d_2d_3-d_1d_4)(d_3-d_4)},S_{12}^{22}=\frac{(-d_1d_4^2+d_2d_3d_4)[(\alpha_2-1)m_{11}+\alpha_3\lambda_{11}]}{a_k^2}$$

$$S_{12}^{23}=\frac{(-d_2d_3^2+d_1d_3d_4)[(\alpha_2-1)m_{22}+\alpha_3\lambda_{22}]}{a_k^2},S_{12}^{24}=\frac{2d_2d_3d_4[(\alpha_2-1)m_{11}+\alpha_3\lambda_{11}]}{a_k^2+(\lambda_{11}h+\lambda_{22}h)^2}$$

$$S_{12}^{25}=\frac{(d_2d_3+d_1d_4)[(\alpha_2-1)d_4m_{11}+\alpha_3d_4\lambda_{11}]}{a_k^2+(2\lambda_{11}h)^2},S_{12}^{26}=\frac{2d_1d_4d_3[(\alpha_2-1)m_{22}+\alpha_3\lambda_{22}]}{a_k^2+(\lambda_{11}h+\lambda_{22}h)^2}$$

$$S_{12}^{27}=\frac{(d_2d_3+d_1d_4)[(\alpha_2-1)d_3m_{22}+\alpha_3d_3\lambda_{22}]}{a_k^2+(2\lambda_{22}h)^2}. \tag{C5}$$

$$S_{21}^{11}=\frac{a_k C_{66}}{2\pi(d_2m_{11}-d_1m_{22})(d_2d_3-d_1d_4)},S_{21}^{12}=\frac{(m_{11}\lambda_{11}-1)(d_1d_2d_4-d_2^2d_3)}{a_k^2}$$

$$S_{21}^{13}=\frac{(m_{22}\lambda_{22}-1)(d_1d_2d_3-d_1^2d_4)}{a_k^2},S_{21}^{14}=\frac{2d_1d_2d_4(m_{11}\lambda_{11}-1)}{a_k^2+(\lambda_{11}h+\lambda_{22}h)^2},$$

$$S_{21}^{15}=\frac{(d_2^2d_3+d_1d_2d_4)(m_{11}\lambda_{11}-1)}{a_k^2+(2\lambda_{11}h)^2},S_{21}^{16}=\frac{(d_1d_2d_3+d_1^2d_4)(m_{22}\lambda_{22}-1)}{a_k^2+(2\lambda_{22}h)^2} \tag{C6}$$

$$S_{21}^{17}=\frac{2d_1d_2d_3(m_{22}\lambda_{22}-1)}{a_k^2+(\lambda_{11}h+\lambda_{22}h)^2}.$$

$$S_{22}^{21}=\frac{C_{66}}{2\pi(d_2d_3-d_1d_4)(d_4-d_3)},S_{22}^{22}=0,S_{22}^{23}=0,$$

$$S_{22}^{24}=\frac{2d_2d_3d_4(\lambda_{11}h+\lambda_{22}h)(1-m_{11}\lambda_{11})}{a_k^2+(\lambda_{11}h+\lambda_{22}h)^2},S_{22}^{25}=\frac{(d_2d_3d_4+d_1d_4^2)(2\lambda_{11}h)(-1+m_{11}\lambda_{11})}{a_k^2+(2\lambda_{11}h)^2},$$

$$S_{22}^{26}=\frac{2d_1d_3d_4(\lambda_{11}h+\lambda_{22}h)(1-m_{22}\lambda_{22})}{a_k^2+(\lambda_{11}h+\lambda_{22}h)^2},S_{22}^{27}=\frac{(d_2d_3^2+d_1d_3d_4)(2\lambda_{22}h)(-1+m_{22}\lambda_{22})}{a_k^2+(2\lambda_{22}h)^2}. \tag{C7}$$

چکیده

مقاله حاضر آنالیز شکست ترکیبی در یک نیم صفحه ارتوروپیک تضعیف شده توسط چندین ترک متحرک می‌باشد. نیم صفحه ارتوتروپیک حاوی نابجایی لبه ای برشی و قائم از نوع ولترا است. محیط تحت بارگذاری درون صفحه‌ای فرض گردیده است. روش توزیع نابجایی برای بدست آوردن معادلات انتگرالی در نیم صفحه ارتوتروپیک تضعیف شده توسط چندین ترک مستقیم استفاده شده است.

در ابتدا با استفاده از تبدیل فوریه مسأله نابجایی حل شده و میدان تنش‌ها بدست آمده اند. معادلات انتگرالی دارای تکینگی از نوع کوشی می‌باشند که با استفاده از روش عددی این معادلات جهت بدست آوردن دانسیته نابجایی روی سطوح ترک‌ها حل گردیده‌اند که در نهایت منجر به محاسبه ضریب شدت تنش در نوک ترک‌ها می‌شوند. چندین مثال عددی برای محاسبه ضرایب شدت تنش مود I و II مکانیک شکست برای نشان دادن اثرات پارامتر ارتوتروپیک، طول ترک و سرعت ترک برای روی آنها حل شده است.